MACHINABILITY ANALYSIS ON WIRE EDM OF 6 WT. % NI-COATED AL2O3P REINFORCED AA7075 MMCS USING TOPSIS

Vijay Praveen[1,3], Ranga Raju[2], Jagannadha Raju[3]

[1] Department of Mechanical Engineering, Bapatla Engineering College, Bapatla, India
[2]Professor, Srinivasa Institute of Engineering and Technology, Amalapuram, India.
[3]Department of Mechanical Engineering, A.U. College of Engineering (A), Vishakhapatnam, India.

Corresponding author: D Vijay Praveen, d.vijay.praveen@gmail.com

Abstract: The current research paper is focused on investigating the influence of Wire-cut EDM process parameters on materials removal rate and surface roughness of 6 weight percentage of nickel coated alumina reinforced AA7075 composite materials. Taguchi's L_{27} multi-level orthogonal array is adopted to conduct the experimental studies. Technique for order preference by similarity to the ideal solution is used to study the optimal combination of the machining process parameters. The combined effect of machining performance measures is analyzed using analysis of variance to identify the significance of the result. The surface morphology of the machined surface of the optimal set of parameters has been studied. Further, optimal parameters are verified by conducting the confirmation tests and the predicted results have been a good agreement with the experimental findings.

Key words: Wire-EDM, Non-conventional machining, Optimization, MRR, Ra, TOPSIS.

1. INTRODUCTION

Metal matrix composites (MMCs) find an extensive assortment of applications in manufacturing industries due to its excellent mechanical properties, low density and good corrosion resistance. Conventional machining of Al-based MMCs is challenging due to the presence of hard reinforced ceramic particles in the material tends to enfold around the tool, which leads to tool damage. These issues became more challenging in the case of conventional machining of metal matrix composites [1]. So the focus was moved to non-conventional machining. Among all, Wire Electrical Discharge Machine (WEDM) is a personal endorsement of the conventional EDM process. It is a non-contact machining process, which is suitable for the productive machining of MMCs regardless of the hardness with an enormous surface finishing with high dimensional accuracy [2]. During the WEDM process, the material will be eroded at the forefront of the electrode wire, and there is no direct contact between the workpiece and the wire electrode. WED machining parameters are to be attuned to attain the utmost material removal rate, cutting speed, dimensional accuracy and good surface quality. The selection of best parameters is not readily available; moreover, differs from material to material. Therefore, there is a considerable demand for identifying the performance parameters for machining a variety of MMCs, super alloys and other advanced materials [3].

Various experimental machining studies were conducted on different materials to analyze the wire EDM machining performance. Karthik et al. worked on WEDM studies of Al/AlCoCrFeNiMo0.5 MMC, which were fabricated by the powder metallurgy technique. They investigated the influence of materials, machining parameters varying parameters like pulse on, pulse off and wire feed. From the ANOVA analysis, they revealed that pulse on time was the most influencing parameter than that of the other variables. TOPSIS technique was used for identifying the optimal combination of the influencing parameters that enhances productivity [4]. Gopal and Soorya prakash [5] had carried out multi objective optimization of WED machining features of novel Mg/BN/CRT Hybrid MMCs using TOPSIS technique. Muniappan et al. [6] investigated the optimal wire electrical discharge machining parameters of SiC/graphite reinforced Al-6061alloy using Taguchi's L_{27} orthogonal array. The optimal combination of parameters was proposed using TOPSIS methodology to minimize the cutting speed and kerf width. Similar studies were carried out on traditional and non-traditional machining processes using various optimization techniques on ceramic particles reinforced MMCs [7-13]. However, there exist some challenges in the fabrication of MMCs, such as bonding, wettability, and interfacial reactions between the metal matrix and reinforced particulates [14]. Metallic coatings on ceramic reinforcement can minimize these problems thereby enhance the physical and mechanical properties of coated particles reinforced MMCs [15-17]. These novel materials have a broad scope in machining studies

using various advanced optimization techniques to improve machining performances.

In this present study, to acquire the advantage of improved features of these novel coated composites, an attempt has been made to carry out the Wire-cut electro-discharge machining study on 6 wt. % of nickel-coated alumina reinforced 7075 MMCs, which interns improve in productivity.

2. MATERIALS AND METHODS

2.1 Preparation of the composites

Aluminum-based Composite materials have become more modern materials as they got superior mechanical properties. AA 7075 has been chosen as matrix alloy, and alumina particles have been selected as reinforcement, owing to their superior physical and mechanical properties. The chemical content of 7075 alloys is Zn 5.6%, Mg 2.3%, Cu 1.5%, Si 0.5%, Mn 0.5%, Ti 0.5%, Cr 0.5% and Al-balance.

The electroless coating technique has been adopted for the coating of the alumina particles, as this coating method has got advantages like simple in operation, uniform plating, and mass production when compared with the other plating methods [16]. Nickel was chosen as plating material and the steps followed were shown in Figure 1.

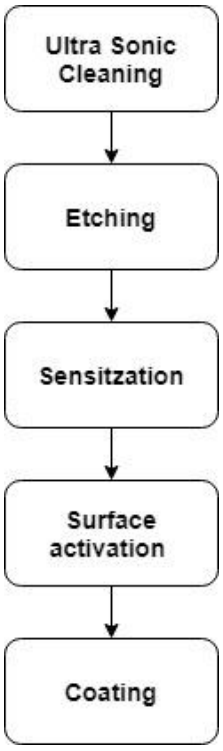

Fig. 1. Steps in EN coating [16]

The nickel coating process on alumina particles has been carried out as per ASTM B-733 standards. Surface treatment and bath preparation are the main steps in the Electro-less coating technique [16]. A detailed procedure of coating, mechanical properties and micro structural characteristics were explained in our earlier work [18].

The standard stir casting route was adopted for the preparation of the composite. The nickel coated particles were initially preheated and introduced in to the hot melt at mechanical stirring speed of 350 rpm for a period of 8 minutes. Melt was finely poured in to the preheated moulds. A weight composition of 6 % was chosen for the present study. The composite have shown better physical, mechanical properties compared to the other weight percentage of reinforcements [18].

2.2 Machining Terms and parameters

As per the apparent literature survey, it can be established that pulse on time (T_{on}), pulse off time (T_{Off}), gap voltage (V), peak current (I) ,wire feed (WF) and wire tension (WT) are vital factors that express the material eminence in WEDM so that these factors are taken as input process parameters. Material removal rate (MRR) and surface roughness (Ra) are always given top priority in machining responses, as productivity always depends upon MRR and Ra. MRR and width of the cut can be calculated using equations (1) and (2).

$$MRR = \text{Mean speed (mm/min)} \times \text{Thickness of material (mm)} \times \times \text{Width of cut (mm)} = V_c \times t \times b \text{ mm}^3/\text{min} \quad (1)$$

$$\text{Width of the cut} = 2 \times \text{spark gap} + + \text{electrode wire diameter} \quad (2)$$

Surface roughness was examined by Surftest SJ-210 (Mitutoyo). Three readings were taken on each side of the machined specimen, and averages of them were considered as the surface roughness of the samples.

3. METHODOLOGY

3.1 Design of Experiments

In the present experimental study, experiments were designed according to Taguchi's L_{27} orthogonal array, using Minitab 18 software with six factors and 3 levels. Parameters with their levels were depicted in Table 1.

Table 1. Factors and levels

Factors	Notation	Levels		
Pulse On (µs)	A	122	124	126
Pulse Off (µs)	B	50	54	58
Gap Voltage (V)	C	30	35	40
Peak Current (A)	D	130	145	160
Wire Feed (m/min)	E	3	4	5
Wire Tension(N)	F	4.9	9.8	14.7

3.2 Analysis of Responses using Taguchi's S/N Ratio

Taguchi's signal–noise (S/N) ratio was used to analyze the measure of machining performance. In the present study, ideal characteristics of material removal rate and surface roughness were determined using this technique. Experimental results were converted to S/N ratio, and higher value denotes better combination parameters. Depending upon the type of quality elements, S/N ratios are calculated, namely nominal the better, smaller the better and larger the better [13]. The material removal rate must be maximized so that larger the best was chosen and determined by using equation (3), and surface roughness with lower the best-using equation (4).

$$SN_{LB} = -10\log_{10}\left(\frac{1}{n}\sum_{i=1}^{n}\left(1/y_i^2\right)\right) \quad (3)$$

$$SN_{SB} = -10\log_{10}\left(\frac{1}{n}\sum_{i=1}^{n}y_i^2\right) \quad (4)$$

3.3 TOPSIS

Technique for order preference by similarity to the ideal solution was developed by Hwang and Yoon. Multi-objective decision-making problems can be solved by using TOPSIS by combining the entire range of performance attribute values being considered for every alternative into one single value. This technique reduces the original problem into a single decision-making problem [19]. The methodology was shown in Figure 2.

Fig. 2. Methodology of TOPSIS

The response of the experimental data should be normalized for getting uniformity of data. The range of normalized values of machining data is zero to one. For the current empirical analysis, Material removal rate (MRR) and surface roughness (Ra) of each set of the experiments are to be normalized for consistency of response using equation (5).

$$M_{ij} = \frac{U_{ij}}{\sqrt{\sum_{i=1}^{x} U^2{}_{ij}}} \quad (5)$$

Where M_{ij} is the normalized decision matrix and U_{ij} is the output value of the alternative.

After determining the normalized data of the machining responses, weighted normalized value must be determined using equation (6).

$$V_{ij} = x_j \times M_{ij} \quad (6)$$

Where:

x_j is the weight of j^{th} criterion.

The positive ideal solution (V^+) and negative ideal solution (V^-) are to be calculated using equation (7) and (8).

$$V^+ = \{(\max V_{ij}) \mid (j\epsilon J), (\min V_{ij} \mid (j\epsilon J^*) \mid i=1,2\ldots27\} \quad (7)$$

$$V^- = \{(\min V_{ij}) \mid (j\epsilon J), (\max V_{ij} \mid (j\epsilon J^*) \mid i=1,2\ldots27\} \quad (8)$$

Where:

J is a set of beneficial attributes and

J* is the set of non-beneficial attributes.

Equation (9) and (10) are used for the separation of each alternative from a positive ideal solution and a negative ideal solution [19].

$$S_i^+ = \left[\sum_{j=1}^{27}\left(V_{ij} - V_j^+\right)^2\right]^{0.5} \quad i = 1,2,...,27 \quad (9)$$

$$S_i^- = \left[\sum_{j=1}^{27}\left(V_{ij} - V_j^-\right)^2\right]^{0.5} \quad i = 1,2,...,27 \quad (10)$$

Closeness coefficient (P_i) of each alternative is to be calculated using equation (11).

$$P_i = \frac{S_i^-}{S_i^+ + S_i^-} \quad (11)$$

The last step in the TOPSIS procedure is ranks are to be assigned to the relative to the closeness to ideal solution [19].

4. RESULTS AND DISCUSSIONS

4.1 Machining study

Experiments were carried out by Sprint-cut Wire-EDM (Electronica India Ltd., India) at CIPET, Vijayawada. 6 wt. % of nickel-coated alumina reinforced AA 7075 MMC with the dimensions of 100 mm x 100 mm x 14 mm plates was taken as workpiece. The workpiece was machined into 10 mm x 10 mm square piece by arranging machining parameters according to the experimental design (L_{27}) and machined specimens were shown in Figure 3. Machining responses MRR and Ra were depicted in Table 2.

Table 2. Experimental results of WEDM

Exp. run	CODED FACTORS						MRR (mm^3/min)	SR (µm)
	A	B	C	D	E	F		
1	122	50	30	130	3	4.9	2.68	2.99
2	122	50	30	130	4	9.8	2.71	2.85
3	122	50	30	130	5	14.7	2.51	2.77
4	122	54	35	145	3	4.9	2.48	2.93
5	122	54	35	145	4	9.8	2.41	2.87
6	122	54	35	145	5	14.7	2.20	2.78
7	122	58	40	160	3	4.9	2.32	2.93
8	122	58	40	160	4	9.8	2.59	2.75
9	122	58	40	160	5	14.7	2.31	2.69
10	124	50	35	160	3	9.8	3.46	3.49
11	124	50	35	160	4	14.7	3.82	3.36
12	124	50	35	160	5	4.9	3.44	3.24
13	124	54	40	130	3	9.8	3.22	3.29
14	124	54	40	130	4	14.7	3.01	3.15
15	124	54	40	130	5	4.9	2.66	3.12
16	124	58	30	145	3	9.8	2.83	3.26
17	124	58	30	145	4	14.7	2.63	3.21
18	124	58	30	145	5	4.9	2.18	3.12
19	126	50	40	145	3	14.7	4.15	3.64
20	126	50	40	145	4	4.9	3.85	3.45
21	126	50	40	145	5	9.8	3.84	3.38
22	126	54	30	160	3	14.7	3.58	3.53
23	126	54	30	160	4	4.9	3.27	3.38
24	126	54	30	160	5	9.8	3.26	3.32
25	126	58	35	130	3	14.7	3.34	3.54
26	126	58	35	130	4	4.9	2.89	3.42
27	126	58	35	130	5	9.8	2.88	3.25

Fig. 3. A view of Machined Specimens

4.2 Analysis of Machining Responses

Machining responses were analyzed using Taguchi's Signal to Noise (S/N) ratio method. The influence of the machining characteristics on performance measures was discussed as follows:

4.2.1 Data Analysis using ANOVA

Analysis of Variance (ANOVA) technique is used to determine the statistical significance of the machining parameters using Minitab software. ANOVA tables of MRR and Ra were depicted in Table 3 and 4. ANOVA tables shows the parameters such as degree of freedom (DF), sum of square (SS),mean of square (MS), Fisher's ratio (F) and probability value (P). Percentage contribution of each individual parameter on machining responses can be identified from the tables.

Table 3. ANOVA Table of MRR data

Source	DF	Seq SS	Adj SS	Adj MS	F-Value	P-Value	Contribution
Pulse On	2	4.2862	4.2862	2.14311	138.33	0.000	53.52%
Pulse Off	2	2.3541	2.3541	1.17703	75.97	0.001	29.39%
Gap Voltage	2	0.2710	0.2710	0.13551	8.75	0.003	3.38%
Peak Current	2	0.2757	0.2757	0.13785	8.90	0.003	3.44%
Wire Feed	2	0.4223	0.4223	0.21113	13.63	0.001	5.27%
Wire Tension	2	0.1826	0.1826	0.09129	5.89	0.014	2.28%
Error	14	0.2169	0.2169	0.01549			2.71%
Total	26	8.0087					100.00%

Table 4. ANOVA Table of Ra data

Source	DF	Seq SS	Adj SS	Adj MS	F-Value	P-Value	Contribution
Pulse On	2	1.62490	1.62490	0.812448	216.67	0.001	86.74%
Pulse Off	2	0.02714	0.02714	0.013570	3.62	0.054	1.45%
Gap Voltage	2	0.00161	0.00161	0.000804	0.21	0.810	0.09%
Peak Current	2	0.00521	0.00521	0.002604	0.69	0.516	0.28%
Wire Feed	2	0.14410	0.14410	0.072048	19.21	0.001	7.69%
Wire Tension	2	0.01787	0.01787	0.008937	2.38	0.129	0.95%
Error	14	0.05250	0.05250	0.003750			2.80%
Total	26	1.87332					100.00%

According to Table 3 Pulse On time, pulse off time, wire feed, peak current, gap voltage and wire tension are the influencing parameters. Table 4 shows that the pulse on time, wire feed, pulse off time are the notable effecting factors than the other parameters on the surface integrity.

4.2.2 Effect of process parameters on MRR

Main effects plots of MRR were furnished in Figure 4. MRR was increased with the increase of pulse on time due to the rising period of sparking. With the increase of gap voltage and peak current superior metal removal rate was identified due to intensified and even distributed spark at the cutting zone [20]. From the plot, it was observed that with the increased pulse off time, MRR was decreased due to reduced spark discharge time and the pieces of work material still got

trapped in the gap, which leads in minimizing the MRR [12, 21].

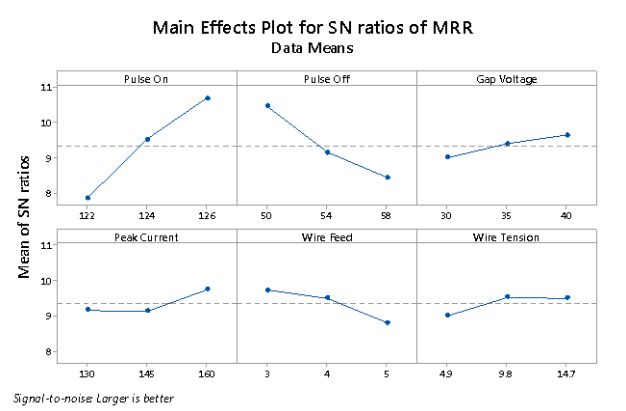

Fig. 4. Main effects plot for Material Removal Rate

There was a small variation in MRR with the increase of wire feed, which may be due to presence of debris and the particulates were stagnated in the gap and further lead to lower MRR [22]. As the load on wire tension increases from 4.9 N to 14.7 N, an increase in the MRR was observed. Spark induced reactive forces and flushing of dielectric in the machining zone causes wire vibrations. These can be minimized by increasing the wire tension, which leads to an increase in MRR [23].

4.2.3 Effect of process parameters on Ra

Effects of pulse on time, pulse off time, gap voltage, peak current, wire feed and wire tension on surface roughness were depicted in Figure 5. As the pulse on-time goes on increasing; high thermal energy will be produced due to influential flare-up on the surface of the material, causing craters produced, which leads to an increase in surface roughness [8, 24]. The better surface finish was observed with the increase of the pulse off time. It's because of increased flushing time and cooling time to tip out more amount of debris, which leads to minimizing the re-solidification of molten material on the machined surface [25]. Peak current and gap voltage have shown a similar response to surface roughness.

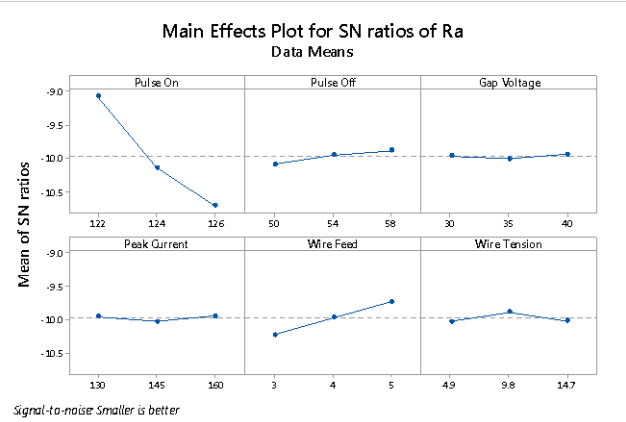

Fig. 5. Main effects plot for Surface Roughness

Initially, surface roughness is decreased with the increase of the peak current and gap voltage up to second level and further decreased. Increased wire feed results in increased surface roughness due to more crater depth, caused by dynamic conditions during the explosion of spark. Wire tension has not shown any significant variation in surface roughness. These results were well agreed with the previous findings by various researchers who have accomplished machining studies for different materials.

4.3 Multi-objective optimization using TOPSIS

In the present study, TOPSIS was chosen for optimizing the combined impact on machining responses. The machining responses (i.e., MRR and Ra) both are having, unlike units. As a result, these measures were normalized according to TOPSIS methodology. Then proceeded for weighted normalized values to determine the closeness coefficient. Calculations of TOPSIS were shown in Table 5.

Table 5. Calculations of TOPSIS

Exp No	Data Normalized Data		Weighted Normalized		Separation Measures		Closeness Co-efficient	Rank
	MRR	Ra	MRR	Ra	MRR	Ra		
1	0.170	0.181	0.085	0.091	0.044	0.069	0.609	17
2	0.172	0.173	0.086	0.086	0.043	0.070	0.619	16
3	0.160	0.168	0.080	0.084	0.049	0.063	0.563	21
4	0.158	0.178	0.079	0.089	0.050	0.063	0.556	22
5	0.153	0.174	0.077	0.087	0.052	0.061	0.536	23
6	0.140	0.169	0.070	0.084	0.059	0.054	0.477	27
7	0.147	0.178	0.074	0.089	0.055	0.058	0.512	24
8	0.165	0.167	0.082	0.083	0.046	0.065	0.585	20
9	0.147	0.163	0.073	0.082	0.055	0.056	0.505	25
10	0.220	0.192	0.110	0.096	0.024	0.091	0.793	7
11	0.243	0.204	0.121	0.102	0.022	0.095	0.814	1
12	0.219	0.196	0.109	0.098	0.026	0.090	0.778	5
13	0.205	0.200	0.102	0.100	0.032	0.084	0.724	10
14	0.191	0.191	0.096	0.096	0.036	0.079	0.688	12
15	0.169	0.189	0.085	0.095	0.046	0.069	0.600	18
16	0.180	0.198	0.090	0.099	0.042	0.074	0.636	15
17	0.167	0.195	0.084	0.097	0.048	0.069	0.589	19
18	0.139	0.189	0.069	0.095	0.061	0.056	0.478	26
19	0.257	0.221	0.129	0.110	0.029	0.091	0.760	4
20	0.245	0.209	0.122	0.105	0.024	0.093	0.796	3
21	0.244	0.205	0.122	0.102	0.022	0.094	0.811	2
22	0.228	0.214	0.114	0.107	0.030	0.089	0.751	6
23	0.208	0.205	0.104	0.102	0.032	0.085	0.723	9
24	0.207	0.201	0.104	0.101	0.032	0.085	0.729	8
25	0.212	0.215	0.106	0.107	0.034	0.085	0.713	11
26	0.184	0.207	0.092	0.104	0.043	0.076	0.638	14
27	0.183	0.197	0.092	0.099	0.041	0.075	0.648	13

From the Table 5, experiment set 11 was observed to be in highest value of closeness co-efficient among in 27 experiments. From these experiments, the optimal combination of the machining parameters are, Pulse on time 124 µs, Pulse off time 50 µs, Gap Voltage 35 V, peak current 160 A, wire feed 4 m/min and wire

tension 14.9 N. So, the optimal settings from the orthogonal array were identified as $A_2B_1C_2D_3E_2F_3$. The mean of closeness co-efficient (CC) of each degree of influencing machining parameters for the present investigation were depicted in Table 6. The difference between maximum and minimum values of the mean of closeness coefficient at each level has also been determined, which is used to determine the rank of parameters.

Table 6. Response Table of Closeness Co-efficient

Machining parameters	Average Closeness coefficient			Max-Min	Rank
	Level 1	Level 2	Level 3		
T_{on}	0.5514	0.6777	**0.7300**	0.1786	1
T_{off}	**0.7270**	0.6427	0.5894	0.1377	2
V	0.6330	0.6614	**0.6647**	0.0317	6
I	0.6446	0.6266	**0.6879**	0.0613	3
WF	**0.6727**	0.6654	0.6210	0.0516	4
WT	0.6322	**0.6757**	0.6512	0.0435	5

From the obtained results, the predicted order parameters are pulse on time, followed by pulse off time, peak current, wire feed, wire tension and gap voltage. The optimal set obtained from the response table can be written as $A_3B_1C_3D_3E_1F_2$.

4.4 Analysis of Variance(ANOVA) for TOPSIS

The effect of machining parameters on performance measures was investigated by ANOVA analysis. In addition to that, F(Fisher's) test and P(probability) value were also determined. In the F- test, higher in F value shows a significant influence on performance measures [26]. ANOVA results were depicted in Table 7.

Table 7. ANOVA analysis for Closeness co-efficient

Source	DF	Adj SS	Adj MS	F-Value	P-Value	% Contribution
Pulse On	2	0.151814	0.075907	78.32	0.000	50.93%
Pulse Off	2	0.086766	0.043383	44.76	0.000	29.11%
Gap Voltage	2	0.005467	0.002734	2.82	0.093	1.83%
Peak Current	2	0.017843	0.008921	9.21	0.003	5.99%
Wire Feed	2	0.014055	0.007027	7.25	0.007	4.72%
Wire Tension	2	0.008573	0.004286	4.42	0.032	2.88%
Error	14	0.013568	0.000969			4.55%
Total	26	0.298086				100.00%

Percentage contribution of the initial parameter, i.e., Pulse on time was found to be 50.93% followed by pulse off-time 29.11%, Peak current 5.99%, wire feed 4.72% and wire tension 2.88%, whereas the least significant parameter, was identified as gap voltage with 1.83% contribution respectively.

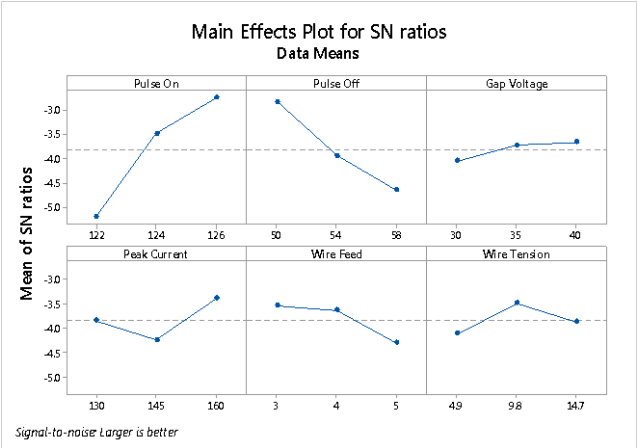

Fig. 6. Main effects plot of Machined specimens

The main effects plot for the S/N ratio of closeness coefficient results were shown in Figure 6. From the main effects plots, improvement in the combined impact of machining responses were identified at a higher pulse on time, gap voltage, peak current. In addition to this, lower pulse off time with a moderate level of wire tension was observed to be a better combination for obtaining the optimal parametric set of MRR and Ra. At these levels of parameters, more erosion occurred due to increased spark energy and better surface integrity, which caused an enhancement in the closeness coefficient.

4.5 Confirmation Tests

The last step in the DOE is to conduct the confirmation tests to validate the ends drawn during the investigation stage. After the assessment of the suitable process parameters setting, a confirmation run is to be carried out. The predicted optimum value of closeness coefficient, 'γ' can be determined using the following equation (12):

$$\gamma = \gamma_k + \sum_{i=1}^{l} \left(\gamma_i - \gamma_k\right) \qquad (12)$$

Where γ_i is the total means of closeness coefficient (CC), γ_k is the mean of optimum level CC and l denotes the number of effecting parameters [21]. Confirmation tests were performed with leading a particular test with a specific set of machining variables, which were assessed recently [21, 27]. Results of the 11th experiment, which was the optimal parameter set from the orthogonal array, predicted the optimal set from closeness coefficient response table and experimental run of predicted set

were illustrated in Table 8.

Table 8. Machining performance results

	Optimal process parameters		
Responses	Optimal set from Orthogonal array (L_{27})	Predicted Optimal set	Confirmation test for Predicted Optimal set
Levels	T_{on}(122) T_{off}(54) V(35) I(145) WF(5) WT(9.8)	T_{on}(126) T_{off}(50) V(40) I(160) WF(3) WT(9.8)	T_{on}(126) T_{off}(50) V(40) I(160) WF(3) WT(9.8)
MRR	3.82	--	3.83
Ra	3.36	--	3.37
Closeness Coefficient	0.816	0.893	0.813

Confirmation experimental runs were conducted upon predicting the optimal parametric set from closeness coefficient response table. Three experimental runs were performed for both MRR and Ra. According to the obtained results, the average value of the material removal rate was slightly decreased from 3.82 mm^3/min to 3.83 mm^3/min, and surface roughness was increased from 3.36 µm to 3.37 µm. From the confirmation test results, it can be revealed that the predicted parameters were found to be the right consistency with the experimental results; hence the predicted optimal parameters were validated.

4.6 Machined Surface Analysis

SEM images along with Energy dispersive x-ray analysis (EDAX) of the machined specimens of optimal runs ($A_1B_2C_2D_2E_3F_2$ and $A_3B_1C_3D_3E_1F_2$) were portrayed in Figure 7. From the images, surface irregularities like craters, micro-cavities,oxide inclusions, debris, and melted deposits were observed. During WEDM, some quantity of melted workpiece is flushed away with dielectric fluid, and leftover melted stuff solidifies on the surface of the workpiece [26].

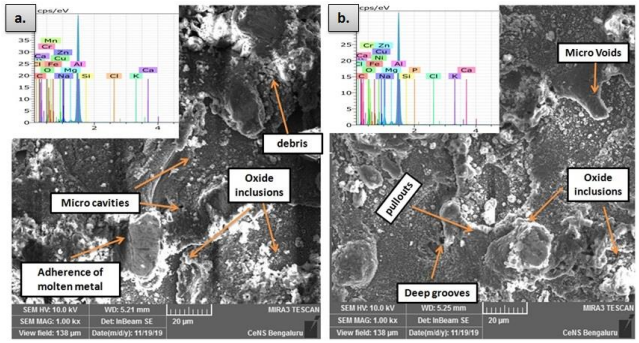

Fig. 7. SEM and EDAX of the machined surface of Exp run (a) $A_1B_2C_2D_2E_3F_2$; (b) $A_3B_1C_3D_3E_1F_2$

This machined surface is mainly influenced by control factors such as pulse on time and peak current. With the increase in pulse on time, the thermal energy relayed to the specimen intensifies and additional material is removed. Furthermore, the development of the plasma channel fallout, ensuing the diminution of plasma flushing efficiency. As a result of this tendency, less quantity of molten metal is washed out by the dielectric [27-28]. Pullouts are formed due to the presence of surface tension in the molten metal. Microcracks and deep grooves are generated due to thermal and tensile stress during the machining process. In addition to the process parameters, material properties like thermal conductivity,thermal expansion, modulus of elasticity and tensile strength also influence the surface integrity of the workpiece while machining [29-31]. At smaller levels of pulse on time and peak current, smaller amount of thermal energy is produced while machining. This results in less amount of heat conduction into the workpiece and lesser volume in MRR. Thus a small amount of debris is observed on the machined surface. Surface abnormalities are more in the predicted optimal set, when compared to experimental run 11 due to higher levels of pulse on time and peak current.

5. CONCLUSIONS

Identifying optimal combinations of the machining parameters is difficult, as the machining process involves various electrical and non-electrical parameters. In the present study, TOPSIS technique based on Taguchi's DOE was adopted to study the optimal parameters for machining the 6 wt. % Nickel-coated alumina reinforced MMCs. The consequences of the machining responses were analyzed using Taguchi's Analysis. The following are conclusions obtained from this exploration:

- The present investigation was modelled as multi-objective optimization, which maximizes the MRR and minimizes the Ra.
- The largest value of closeness coefficient has a high impact on the machining, as compared with the other parameters. Experimental run 11, i.e. T_{on}=130 µsec, T_{off}=55 µsec, Gap Voltage=40 V, Peak current=180 A, wire feed=2 m/min, and wire tension= 9.81 N were found to be the best parameters.
- The predominance of considered input process parameters on the performance characteristics was divulged by the adopted TOPSIS by selecting suitable and well balanced experimental runs.
- From ANOVA, it is made known that pulse-on-time, pulse off time, peak current and wire feed are the most significant parameters for desired performance characteristics.

The discussed Taguchi based TOPSIS methodology

in the present investigation is most appropriate for establishing the best combination of the process parameter, to attain enrichment in machining performance of Ni-coated Al_2O_3/7075 alloy.

6. REFERENCES

1. Amini, H., Soleymani Yazdi, M. R., & Dehghan, G. H. (2011). *Optimization of process parameters in wire electrical discharge machining of TiB2 nanocomposite ceramic*. Proceedings of the Institution of Mechanical Engineers, Part B: Journal of Engineering Manufacture, **225**(12), pp. 2220-2227.
2. Praveen, D. V., Raju, D. R., Raju, M. J. (2020). *Optimization of machining parameters of wire-cut EDM on ceramic particles reinforced Al-metal matrix composites–A review*. Materials Today: Proceedings, **23**, doi:10.1016/j.matpr.2019.05.392.
3. Muralidharan, N., Chockalingam, K., Parameshwaran, R., Kalaiselvan, K., Nithyavathy, N. (2020). *Optimization of CNC-WEDM Parameters for AA2024/ZrB2 in situ Stir Cast Composites Using Response Surface Methodology with Desirability Function Technique*. Arabian Journal for Science and Engineering, **45**(7), pp. 5563-5579.
4. Karthik, S., Prakash, K. S., Gopal, P. M., Jothi, S. (2019). *Influence of materials and machining parameters on WEDM of Al/AlCoCrFeNiMo0. 5 MMC*. Materials and Manufacturing Processes, **34**(7), pp. 759-768.
5. Gopal, P. M. (2019). *Wire electric discharge machining of silica rich E-waste CRT and BN reinforced hybrid magnesium MMC*. Silicon, **11**(3), pp. 1429-1440.
6. Muniappan, A., Jaivaakheish, A. P., Jayakumar, V., Arunagiri, A., Senthilkumar, R. (2018). *Multi objective optimization of process parameters in WEDM of aluminum hybrid composite using taguchi and topsis techniques*. Series: Materials Science and Engineering, **402**, 012002.
7. Dey, A., Pandey, K. M. (2018). *Wire electrical discharge machining characteristics of AA6061/cenosphere as-cast aluminum matrix composites*. Materials and Manufacturing Processes, **33**(12), pp. 1346-1353.
8. Pramanik, A., Islam, M. N., Boswell, B., Basak, A. K., Dong, Y., Littlefair, G. (2018). *Accuracy and finish during wire electric discharge machining of metal matrix composites for different reinforcement size and machining conditions*. Proceedings of the Institution of Mechanical Engineers, Part B: Journal of Engineering Manufacture, **232**(6), pp. 1068-1078.
9. Rahman, M., Dey, A., Pandey, K. M. (2018). *Machinability of cenosphere particulate–reinforced AA6061 aluminium alloy prepared by compocasting*. Proceedings of the Institution of Mechanical Engineers, Part B: Journal of Engineering Manufacture, **232**(14), pp. 2499-2509.
10. Lal, S., Kumar, S., Khan, Z. A., Siddiquee, A. N. (2015). *Optimization of wire electrical discharge machining process parameters on material removal rate for Al7075/SiC/Al2O3 hybrid composite*. Proceedings of the Institution of Mechanical Engineers, Part B: Journal of Engineering Manufacture, **229**(5), pp. 802-812.
11. Rao, T. B., Krishna, A. G. (2014). *Selection of optimal process parameters in WEDM while machining Al7075/SiCp metal matrix composites*. The International Journal of Advanced Manufacturing Technology, **73**(1-4), pp. 299-314.
12. Bobbili, R., Madhu, V., Gogia, A. K. (2013). *Effect of wire-EDM machining parameters on surface roughness and material removal rate of high strength armor steel*. Materials and Manufacturing Processes, **28**(4), pp. 364-368.
13. Satishkumar, D., Kanthababu, M., Vajjiravelu, V., Anburaj, R., Sundarrajan, N. T., Arul, H. (2011). *Investigation of wire electrical discharge machining characteristics of Al6063/SiC p composites*. The International Journal of Advanced Manufacturing Technology, **56**(9-12), pp. 975-986.
14. Pillai, T. R. R., Pai, B. C. (1998). *Review Reinforcement coatings and interfaces in aluminium metal matrix composites*. Journal of Material Science, **33**(14), pp. 3491-3503.
15. Ramesh, C. S., Keshavamurthy, R., Channabasappa, B. H., Ahmed, A. (2009). *Microstructure and mechanical properties of Ni–P coated Si_3N_4 reinforced Al6061 composites*. Materials Science and Engineering: A, **502**(1-2), pp. 99-106.
16. Kumar, D. S., Suman, K. N. S., Kumar, P. R. (2016). *A study on electroless deposition of nickel on nano alumina powder under different sensitization conditions*. International Journal of Advanced Science and Technology, **97**, pp. 59-68.
17. Kumar, D. S., Suman, K. N. S., Poddar, P. (2017). *Effect of particle morphology of Ni on the mechanical behavior of AZ91E-Ni coated nano Al2O3 composites*. Materials Research Express, **4**(6), 066505.
18. Praveen, D. V., Raju, D. R., Raju, M. J. (2019). *Influence of nickel coating of Al_2O_3 (P) reinforced AA-7075 metal matrix composites on hardness, impact strength and tensile properties*. Materials Research Express, **6**(12), 126537.
19. Kumar, A., Rai, R. N. (2020). *Grey-Taguchi and TOPSIS-Taguchi-Based Optimisation of Performance Parameters of Spark EDM on Heat-Treated AA7050/5 B 4 C Composite*. Journal of The Institution of Engineers (India): Series D, **101**(1), pp. 71-79.
20. Jailani, H. S., Rajadurai, A., Mohan, B., Kumar, A. S., Sornakumar, T. (2009). *Multi-response*

optimisation of sintering parameters of Al–Si alloy/fly ash composite using Taguchi method and grey relational analysis. The International Journal of Advanced Manufacturing Technology, **45**(3-4), 362.
21. Dhas, D. E. J., Velmurugan, C., Wins, K. L. D. (2018). *Investigations on the effect of tungsten carbide and graphite reinforcements during spark erosion machining of aluminium alloy (AA 5052) hybrid composite*. Silicon, **10**(6), pp. 2769-2781.
22. Lal, S., Kumar, S., Khan, Z. A., Siddiquee, A. N. (2014). *Wire electrical discharge machining of AA7075/SiC/Al 2 O 3 hybrid composite fabricated by inert gas-assisted electromagnetic stir-casting process.* Journal of the Brazilian Society of Mechanical Sciences and Engineering, **36**(2), pp. 335-346.
23. Bhattacharyya, B., Doloi, B. (2019). *Modern Machining Technology: Advanced, Hybrid, Micro Machining and Super Finishing Technology*. Academic Press.
24. Saha, S. K., Choudhury, S. K. (2009). *Experimental investigation and empirical modeling of the dry electric discharge machining process*. International Journal of Machine Tools and Manufacture, **49**(3-4), pp. 297-308.
25. Vijayabhaskar, S., Rajmohan, T. (2019). *Experimental investigation and optimization of machining parameters in WEDM of nano-SiC particles reinforced magnesium matrix composites*. Silicon, **11**(4), pp. 1701-1716.
26. Shahbazi Dastjerdi, M., Mokhtarian, A., Saraeian, P. (2020). *The effect of alumina powder in dielectric on electrical discharge machining parameters of aluminum composite A413-Al 2 O 3 by the Taguchi method, the signal-to-noise analysis and the total normalized quality loss*. International Journal of Mechanical and Materials Engineering, **15**, pp. 1-11.
27. Dhobe, M. M., Chopde, I. K., Gogte, C. L. (2013). *Effect of heat treatment and process parameters on surface roughness in wire electro discharge machining*. Int. J. Mech. Eng. & Rob. Res, **2**(2), pp. 275-281.
28. Ikram, A., Mufti, N. A., Saleem, M. Q., Khan, A. R. (2013). *Parametric optimization for surface roughness, kerf and MRR in wire electrical discharge machining (WEDM) using Taguchi design of experiment.* Journal of Mechanical Science and Technology, **27**(7), pp. 2133-2141.
29. Praveen, D. V., Raju, D. R., Raju, M. J. (2021). *Assessment of Optimal Parameters of Wire EDM on Ni-Coated Al 2 O 3p/AA7075 MMCs Using PCA Coupled GRA*. Arabian Journal for Science and Engineering, pp. 1-14.
30. Sonawane, S. A., Kulkarni, M. L. (2018). *Optimization of machining parameters of WEDM for Nimonic-75 alloy using principal component analysis integrated with Taguchi method*. Journal of King Saud University-Engineering Sciences, **30**(3), pp. 250-258.
31. Praveen, D. V., Raju, D. R., Raju, M. J. (2021). *Investigation on Wear Properties of Nickel-Coated Al_2O_{3P}-Reinforced AA-7075 Metal Matrix Composites Using Grey Relational Analysis*. Trends in Mechanical and Biomedical Design, pp. 819-829.

Received: April 03, 2021 / Accepted: June 15, 2021 / Paper available online: June 20, 2021